



Long-Term Trends and Impact of SARS-CoV-2 COVID-19 Lockdown on the Primary Productivity of the North Indian Ocean

*N. Sunanda*¹, *J. Kuttippurath*^{1*}, *R. Peter*¹, *Kunal Chakraborty*² and *A. Chakraborty*¹

¹ CORAL, Indian Institute of Technology Kharagpur, Kharagpur, India, ² Indian National Centre for Ocean Information Services, Ministry of Earth Sciences, Hyderabad, India

OPEN ACCESS

Edited by:

Domenico D'Alelio,
University of Naples Federico II, Italy

Reviewed by:

Qingyou He,
South China Sea Institute
of Oceanology, China
Simona Saviano,
University of Naples Parthenope, Italy

*Correspondence:

J. Kuttippurath
jayan@coral.iitkgp.ac.in

Specialty section:

This article was submitted to
Global Change and the Future Ocean,
a section of the journal
Frontiers in Marine Science

Received: 18 February 2021

Accepted: 29 July 2021

Published: 30 August 2021

Citation:

Sunanda N, Kuttippurath J,
Peter R, Chakraborty K and
Chakraborty A (2021) Long-Term
Trends and Impact of SARS-CoV-2
COVID-19 Lockdown on the Primary
Productivity of the North Indian
Ocean. *Front. Mar. Sci.* 8:669415.
doi: 10.3389/fmars.2021.669415

COrona Virus Disease (COVID) 2019 pandemic forced most countries to go into complete lockdown and India went on complete lockdown from 24th March 2020 to 8th June 2020. To understand the possible implications of lockdown, we analyze the long-term distribution of Net Primary Productivity (NPP) in the North Indian Ocean (NIO) and the factors that influence NPP directly and indirectly, for the period 2003–2019 and 2020 separately. There exists a seasonal cycle in the relationship between Aerosol Optical Depth (AOD), Chlorophyll-a (Chl-a) and NPP in agreement with the seasonal transport of aerosols and dust into these oceanic regions. In Arabian Sea (AS), the highest Chl-a (0.58 mg/m³), NPP (696.57 mg/C/m²/day) and AOD (0.39) are observed in June, July, August, and September (JJAS). Similarly, maximum Chl-a (0.48 mg/m³) and NPP (486.39 mg/C/m²/day) are found in JJAS and AOD (0.27) in March, April, and May (MAM) in Bay of Bengal. The interannual variability of Chl-a and NPP with wind speed and Sea Surface Temperature (SST) is also examined, where the former has a positive and the latter has a negative feedback to NPP. The interannual variability of NPP reveals a decreasing trend in NPP, which is interlinked with the increasing trend in SST and AOD. The analysis of wind, SST, Chl-a, and AOD for the pre-lockdown, lockdown, and post lockdown periods of 2020 is employed to understand the impact of COVID-19 lockdown on NPP. The assessment shows the reduction in AOD, decreased wind speeds, increased SST and reduced NPP during the lockdown period as compared to the pre-lockdown, post-lockdown and climatology. This analysis is expected to help to understand the impact of aerosols on the ocean biogeochemistry, nutrient cycles in the ocean biogeochemical models, and to study the effects of climate change on ocean ecosystems.

Keywords: North Indian Ocean, primary productivity, chlorophyll-a, COVID-19 lockdown, climate change

HIGHLIGHTS

- Assessment of NPP changes in the North Indian Ocean in view of COVID-19 lockdown.
- NPP exhibits negative anomaly in Arabian Sea (AS) and Bay of Bengal (BoB) in 2020.
- SST anomalies are positive in northern AS and BoB during the lockdown.
- AOD anomalies are negative during the lockdown period due to lesser emissions.

INTRODUCTION

About half of the global net oceanic primary productivity (NPP) is contributed by the phytoplankton (Field et al., 1998; Käse and Geuer, 2018). Compared to the terrestrial NPP, the biomass of primary production is about 500 times smaller because the phytoplankton is invariably utilized by the marine food chain (Webb, 2019). The major environmental drivers of oceanic NPP are light, nutrients and temperature. These are, in turn, altered by the changes in associated oceanic and atmospheric processes, and are sensitive to the changes and variability of climate (Field et al., 1998; Chavez et al., 2011). A few of the Essential Climate Variables (ECVs) identified by the Global Climate Observation System (GCOS, 2011) are surface winds, phytoplankton, SST, and aerosols, which are either directly or indirectly connected to the amount of regional and global oceanic NPP.

It has been observed that the average rise in earth surface temperature is about 1.5°C in the past century (IPCC, 2018) and aerosols, the tiny suspended particles in the atmosphere, have also a significant role in this warming or modification of global surface temperatures. The aerosols have been influencing the earth radiation budget in several different ways, and have been studied widely in the past (e.g., Wielicki et al., 1998; Sathesh et al., 2006). To understand the response of oceans to climate change, it is crucial to study the changes in ECVs individually as well as their inter-relationships, feedback between them and their connection to NPP. Previous studies show a positive (Martin et al., 1994; Jickells et al., 2005; Patra et al., 2007; Banerjee and Prasanna Kumar, 2014), negative (Mallet et al., 2009; Paytan et al., 2009; Jordi et al., 2012) and even no correlation between aerosols and oceanic NPP at different world oceanic regions (Cropp et al., 2005; Gallisai et al., 2014).

The intense upwelling during the summer monsoon and convection during the winter monsoon enhances primary productivity in the Arabian Sea (Banerjee and Prasanna Kumar, 2014). The injection of nutrient rich water into the euphotic zone makes Arabian Sea (AS) highly productive, which is unlikely in Bay of Bengal (BoB) due to high stratification there (Prasanna Kumar et al., 2002). Although not highly productive like AS, BoB is subjected to high new production and more structured in removing atmospheric CO₂ on longer time scales (Kumar et al., 2004). Even when there is the availability of nutrients, increased riverine flux reduces the light penetration to depths and thereby restricts NPP in the summer and fall inter-monsoon months (Prasanna Kumar et al., 2010). The dependency of

productivity on insolation is a major factor in the tropical oceans. The wind stirring is also a key factor for primary production in the Indian Ocean (Beaufort et al., 1997). Seasonal changes in the productivity related to nutrient and phytoplankton abundance are crucial for predicting Hilsa habitat and their migratory patterns in the deltaic regions and shelf of BoB (Hossain et al., 2020). The study of NPP in northeast (NE) BoB for the past 26,000 years reveals that the NPP is controlled by nutrient contents and their distribution within the upper water column (Zhou et al., 2020).

Despite being located in similar geographical locations, AS and BoB exhibit different physical and biological characteristics (Prasanna Kumar et al., 2002; Shenoj et al., 2002; Chakraborty et al., 2020). It is primarily due to the southwest monsoon winds where the AS encounters strong upwelling when rapid surface cooling occurs because of entrainment pushed by the strong winds (Findlater, 1969). Nevertheless, the excess precipitation over evaporation and extensive river runoff (Subramanian, 1993) make BoB strongly stratified. These differences are held to be responsible for the physical, chemical, and biological differences between the basins (Kumar et al., 1995).

Several studies have accounted for the distribution of aerosol (Li and Ramanathan, 2002) and their possible connection with Chl-a abundance (Vinayachandran et al., 2004). The sea surface cooling is responsible for injecting nutrients to the surface in the winter monsoon in the northeastern AS, which helps them sustain the primary productivity even after the monsoon (Madhupratap et al., 1996). The connection between phytoplankton bloom and dust deposition over Central AS was analyzed by Banerjee and Prasanna Kumar (2014) and found that blooms cannot be fully described by injection of nutrients by processes such as advection and mixing in the upper ocean. Shafeeque et al. (2017) compared the seasonal cycles of phytoplankton with SST, Aerosol Optical Depth (AOD), and winds off Somalia. The productivity in the high-nutrient low chlorophyll (HNLC) regions of oceans is directly affected by the iron supply (Jickells et al., 2005). Henceforth, altering nutrient types and amounts may change phytoplankton species and their composition and growth rate, and the resultant NPP (Howarth, 1988; Moore et al., 2013). Although the relationship between anthropogenic aerosols on the carbon cycle and climate change is not well understood, it is estimated that nutrient intake due to atmospheric deposition is increasing the CO₂ uptake (Mahowald et al., 2017).

Satellite data are excellent tools for examining global changes in atmospheric pollution, aerosols and primary productivity. The shortwave infrared (SWIR) bands facilitate vigorous atmospheric corrections in coastal turbid waters (Wang et al., 2009), whereas the band around 685 nm is more advantageous for the detection of phytoplankton fluorescence (Gower et al., 1999; Hu et al., 2005). Here, we examine the primary productivity in BoB and AS, and its drivers for the period 2003–2020. We investigate the Chlorophyll-a (Chl-a) variability in different seasons with respect to surface winds, Sea Surface Temperature (SST) and AOD in these oceanic basins. We estimate the NPP using the surface Chl-a, SST, Photosynthetically Active Radiation (PAR), and length of the day (Behrenfeld and Falkowski, 1997). On top of this, we

assess the impact of lockdown, due to the spread of Severe Acute Respiratory Syndrome (SARS) COrona VIRus Disease (COVID) 2019, on AOD and NPP. The long-term analysis of NPP and its drivers will be used to assess the lock-down situation and its impact on NPP.

MATERIALS AND METHODS

Data

We have used the Modern-Era Retrospective analysis for Research and Applications (MERRA-2) Aerosol Optical Depth for the period January 2003–December 2020. These data have a spatial resolution of $0.625^\circ \times 0.5^\circ$ (Global Modeling and Assimilation Office (GMAO), 2015). The satellite-based bias-corrected and merged Ocean Color Climate Change Initiative (OC-CCI) version 4.2 data are taken for the Chl-a measurements (Sathyendranath et al., 2020). The OC-CCI data consist of [MEdium Resolution Imaging Spectrometer–MERIS: 2002–2012, MODIS on Aqua: 2002–to date, and Sea-viewing Wide Field-of-view Sensor (SeaWiFS): 1997–2010] satellite measurements on a 4×4 km resolution for the period 1997–2020. The daily surface winds (at 10 m) and SST were taken from the European Centre for Medium Range Weather Forecast's (ECMWF) Reanalyses, ERA5 data of 25×25 km resolution for the period from 2003 to 2020 (Hersbach et al., 2020). The NPP calculation is carried out using monthly data of Photosynthetically Active Radiation (Goddard Space Flight Center (NASA) et al., 2018), SST (Werdell et al., 2013) from MODIS–Aqua for the period from 2003 to 2020 at 4 km resolution. We started our analysis from the year 2003 because MODIS–Aqua data are continuous from that year onward. Further details of the datasets are provided in **Table 1**.

Methods

The analysis has been carried out for the period 2003–2019, but we have also considered the year 2020 to examine the impact of COVID-19 lockdown on primary productivity. We have divided the year 2020 into three periods: pre-lockdown (1 January–24 March), lockdown (25 March–7 June), and post-lockdown (8 June–30 June). We have analyzed SST, winds, AOD and Chl-a for these periods. We have also analyzed the temporal variability of Chl-a, AOD and NPP separately for the year 2020 and for the period 2003–2019, and made a comparison between both analyses to assess the effect of lockdown on NPP. The NPP is calculated using the equation,

$$NPP = Chl - a \times pb_{opt} \times daylength \times \left[\frac{0.66125 \times par}{(par + 4.1)} \right] \times z_{eu}$$

where Chl-a is Chlorophyll concentration in mg/m^3 , pb_{opt} is the maximum carbon fixation rate within a water column ($mgC/mgChl/hr$), day length is the number of hours of daylight at the given location and NPP is milligrams of carbon fixed per day unit volume, par is the Photosynthetically Active Radiation (PAR) and z_{eu} is the euphotic depth.

Further details about the NPP calculations are provided in Behrenfeld and Falkowski (1997). We have also made a seasonal analysis of Chl-a, AOD, SST overlaid with winds and NPP from 2003 to 2019 to understand the variability of these variables over the North Indian Ocean (NIO). The seasons are divided according to the classification of the India Meteorological Department. They are: Winter monsoon: January and February (JF), Pre-monsoon: March, April and May (MAM), Monsoon: June, July, August and September (JJAS) and Post-monsoon: October, November and December (OND).

Our analysis is mainly divided into two parts: one is the spatial analysis over the whole NIO region and temporal analysis over selected regions. First, we made a climatology using monthly data from the year 2003 to 2019. To examine the impact of COVID-19, we have made use of daily data because we are focusing on three periods and compared them with the monthly climatology. We have done the analysis for the same period, i.e., pre-lockdown, lockdown and post-lockdown for the year 2018 for comparison. We calculated the anomaly of these periods from the climatology of 17 years (2003–2019) and repeated the same for 2018. We have also chosen three concentric regions in the BoB, which are described in **Supplementary Table 1**. These areas are depicted in **Figure 1**.

The wind stress (WS) is calculated using,

$$\tau = \rho_{air} * Cd * |U|^2$$

where,

$\rho_{air} = 1.225$ kg/m^3 , $Cd = 0.0013$, and U is the magnitude of wind.

We have analyzed the pixel-wise spatial trend of SST, WS, AOD, Chl-a, and NPP from 2003 to 2019. We have computed the spatial trend to analyze the patterns with respect to recent years. We select two regions in BoB and AS, which represent the positive/negative spatial trend of NPP to depict the interannual variability of Chl-a, SST, WS, AOD, and NPP. This interannual variability is represented as a box plot that has two parts; different quartiles and two whiskers.

RESULTS

Chl-a, AOD, and SST and Their Relationship With NPP

When we consider the effects of atmospheric deposition on the phytoplankton abundance, it is also necessary to assess the impact of global land surface and oceanic warming. **Figure 1** shows the monthly SST climatology overlaid by 10 m wind vectors. The tropical Indian Ocean SST has a major role in the climate and its regional variability (Chowdary et al., 2015; Kuttippurath et al., 2021a) and its variability in global scales (Schott et al., 2009). The monthly analysis of SST shows a primary peak in May and a secondary peak in November, and the seasonal reversal of winds associated with the SW (southwest) and NE monsoons (Webster et al., 1998). The observed annual cycle in AS shows two modes of SST seasonality with the primary peak during April–May and the secondary peak in October (Vinayachandran and Shetye, 1991;

TABLE 1 | Details of datasets used in this study.

Sl. No.	Variable	Dataset	Temporal coverage	Spatial resolution
1	SST	ERA5	2003–2020	25 km × 25 km
2	Chl-a	OC-CCI	2003–2020	4 km × 4 km
3	AOD	MERRA-2	2003–2020	0.625 × 0.5°
4	SST (for NPP calculation)	MODIS-Aqua	2003–2020	4 km × 4 km
5	PAR (for NPP calculation)	MODIS-Aqua	2003–2020	4 km × 4 km

Murtugudde and Busalacchi, 1999; Fathrio et al., 2017). During April–May, prior to the onset of Indian summer monsoon, AS is one of the warmest regions in the tropical oceans (Joseph et al., 2006). The seasonal SST cycle is very prominent in BoB, with maxima in May and October (Rahaman et al., 2020). The three concentric box regions are chosen for further discussion (Prakash et al., 2012).

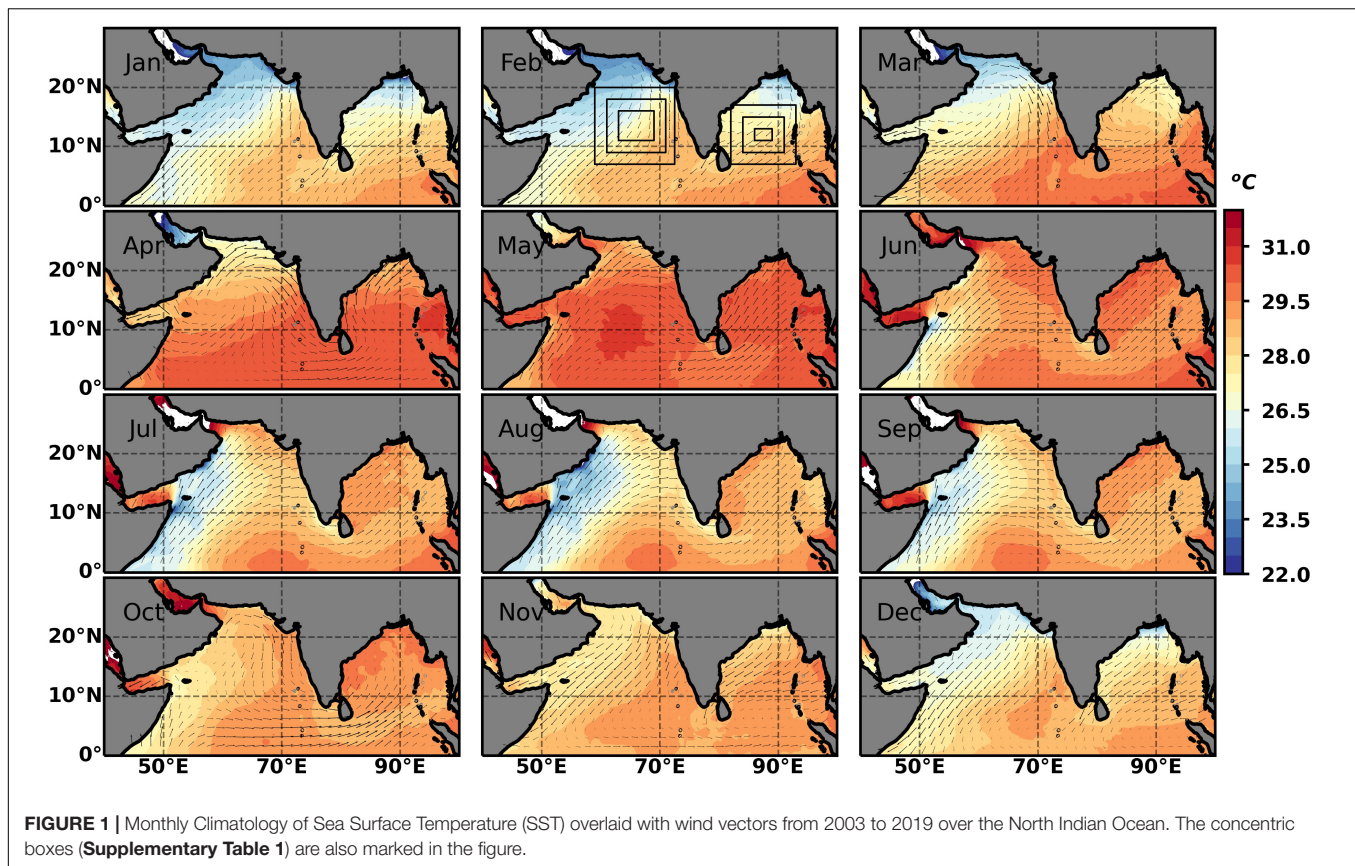
Figure 2 shows the seasonal variation of AOD, Chl-a, NPP and WS over NIO. Surrounded by several deserts, AS is characterized by higher AOD which peaks in JJAS. The concentration of AOD again increases in OND, and the minimum aerosol loading is observed in JF. In BoB, the highest concentration of AOD is observed in MAM in the northern Bay and lowest in OND. In southern BoB, AOD concentrations remain about 0.25 – 0.3 across all the seasons. There are two peaks in AS, one in MAM and the other in JJAS (Kuttippurath and Raj, 2021). However, our analyses reveal the highest concentration of AOD in JJAS although small regions depict an aerosol concentration of 0.4–0.5 in the south eastern AS during MAM. The first peak is due to continental air mass carried to sea by prevailing north-easterly winds (e.g., Ramachandran and Jayaraman, 2002). The second peak is the result of transport of land-originated aerosols from northern Africa and Gulf regions (e.g., Patra et al., 2005). The highest average AOD in AS is about 0.39 in JJAS and lowest in JF of about 0.203. In BoB, the highest AOD is about 0.27 in MAM and lowest in OND of about 0.2. The basin-averaged values in different seasons are listed in **Supplementary Table 2**. The source of aerosols over BoB is mostly from the Indian Subcontinent (e.g., Moorthy et al., 2003). It is also necessary to understand that the aerosols from the northern Africa and Gulf regions are naturally formed desert dust or sand (Prospero et al., 2002). In contrast, those produced in the Indian subcontinent are mostly anthropogenic and composed mainly of black carbon (soot) and fly ash originated due to the fossil fuel combustion and biomass burning (Ramanathan et al., 2001; Prospero et al., 2002).

The AS shows higher concentrations of Chl-a than those over BoB in all months and the smallest difference is observed during MAM, as shown in **Figure 2**. The northeastern AS has the highest concentrations throughout the year with the least seasonal variability, whereas contrasting characteristics are exhibited by the southern AS with significant seasonal changes. The northwest AS shows high Chl-a concentration during JJAS. The northern AS depicts higher concentration of Chl-a in JF, whereas over the rest of AS, the Chl-a remains marginally small. During the pre-monsoon season, the southern regions exhibit relatively smaller concentrations of Chl-a. With the advent of monsoon in JJAS, the southern AS show higher amounts of

Chl-a, particularly in the SW and some parts of SE regions. The seasonality of Chl-a in the southern regions is prominent, but the northern AS remains nearly similar in all months. In BoB, the Chl-a concentration shows 0.2–0.4 mg/m³ smaller than that in AS throughout the year. The northern BoB shows small seasonal variability compared to that of the southern BoB. However, BoB shows the highest concentration of Chl-a in JJAS followed by OND, JF and the smallest in MAM. There is an increase in Chl-a in JJAS near Sri Lankan coast, associated to the upwelling along the southwest coast of India and transport by the monsoonal currents (Vinayachandran et al., 2004; Chakraborty et al., 2018). The southwest BoB shows a higher concentration of Chl-a than that of the southeast BoB with increasing its concentration from OND to JF. The magnitude of Chl-a in AS is higher in NW, and then it gradually decreases with NE, SW, and SE regions (Patra et al., 2007). The highest average Chl-a concentration is about 0.58 mg/m³ in AS and 0.48 mg/m³ in BoB.

The biological activity of AS is influenced by intense seasonal activity of the atmospheric circulation resulting in strong upwelling along the west coast and series of entrainments forced by winds in the central AS (McCreary et al., 2009). The NPP has a spatial pattern similar to that of Chl-a. The NW region of AS shows high NPP close to 1000 mgCm²/day during JF, while the NPP is significantly smaller during MAM, coinciding with the smaller Chl-a there. It is also important to note that the primary peak of SST in AS occurs in MAM, which may be one of the reasons for the smaller primary productivity over AS in this period. The NW and SW regions of AS exhibit high productivity during JJAS. The upward Ekman pumping and coastal upwelling drive the increased productivity in the western coastal AS (Anderson and Prell, 1992; Anderson et al., 1992). Therefore, productivity in the central and northern AS also increases during the SW monsoon (Keen et al., 1997; Prasanna Kumar et al., 2001; Caley et al., 2011). The mixing and WS in the upper layers, as well as the Ekman pumping generated by the positive WS curl, lead to the advection of nutrients to the surface layers to enhance NPP in these regions (Lee et al., 2000; Prasanna Kumar et al., 2001; Wiggert et al., 2005). The Chl-a and WS exhibit a positive relationship and prominent seasonal cycle in AS and BoB with a peak WS of 0.11 and 0.08 in JJAS. The changes in the WS and its curl can condition the biological productivity, and as such, there is no straight connection between boreal summer productivity and summer monsoon intensity (Le Mézo et al., 2017). NPP show comparatively smaller values in BoB except near Sri Lanka in JJAS.

The spatial variability of SST, WS, AOD, Chl-a, and NPP reveals varying trends over different NIO regions (**Figure 3**). In

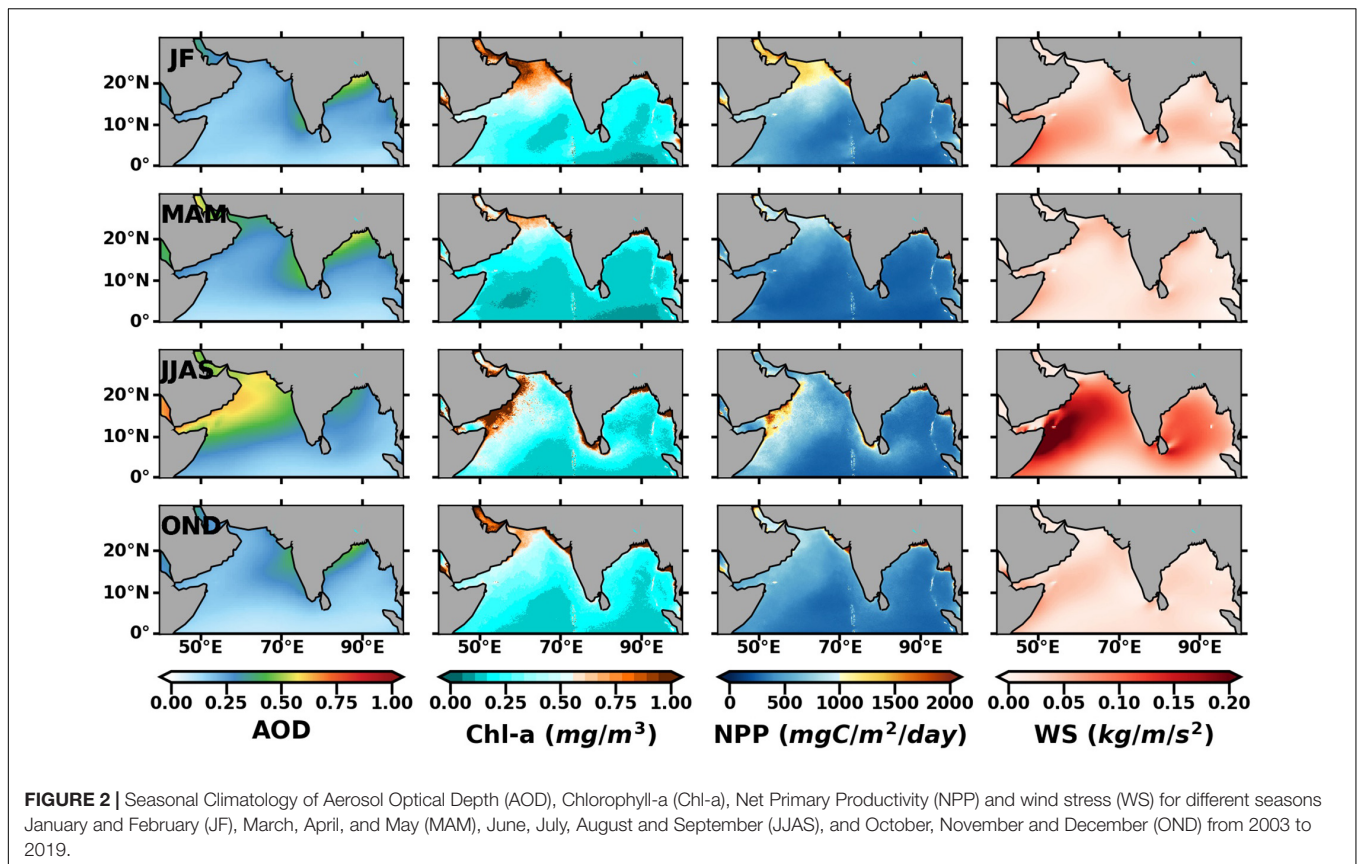


AS, there is a significant increasing trend of AOD in the northern and southern regions particularly in the central and western parts. The western BoB also shows a significant increasing trend whereas an insignificant decreasing trend in the southern BoB. Even though the southern parts of AS and BoB show a noticeable warming trend in SST, the northern parts show an insignificant decreasing trend. The Chl-a shows a decreasing trend in the regions where SST shows an increasing trend. A similar variability is also observed for NPP. Nevertheless, the rising trend of NPP for the regions with suppressed warming highlights the role of physical processes in controlling the phytoplankton dynamics. There is a decelerating trend of NPP and Chl-a in the AS, except for some small regions in the northeastern coast of AS, but an increasing trend in Chl-a and NPP in the southern BoB. It highlights the recent warming and the change in stratification causing the enhancement of the phytoplankton and NPP in recent years. Over the past few decades, there has been an increase in the Chl-a concentration in the coastal waters around the world (Goes et al., 2005; Gregg et al., 2005) and in the oceanic heat content (Levitus et al., 2000). The nutrients exhibit a decreasing trend in the western and an increasing trend in the southeast Indian Ocean, where the warming is not prominent. In this context, the atmospheric deposition is more critical for triggering NPP (Patra et al., 2007). The changing monsoonal circulation and winds (Roxy et al., 2015) also affect the phytoplankton dynamics because it affects the upwelling mechanism (Goes et al., 2005). Even though the values of NPP and Chl-a show small values in

BoB compared to that in AS, an accelerating trend in NPP and Chl-a is observed in BoB.

The Interannual Variability of NPP Interannual Variability

We have considered three concentric box regions in AS and BoB to understand the interannual variability of Chl-a, AOD and NPP (presented in **Supplementary Figures 1, 2**). The Chl-a is more abundant in AS compared to BoB, whereas AOD shows similar values over AS and BoB. The seasonal cycle of Chl-a is more prominent and well developed in AS than in BoB. The increasing/decreasing abundances in Chl-a is also linked to El-Niño Southern Oscillation (ENSO), Indian Ocean Dipole (IOD) episodes and linked to the passage of cyclones (Kuttippurath et al., 2021b), but we do not focus on those events here, as those are beyond the scope of this study. Instead, we concentrate on the interannual variability of Chl-a and AOD over AS and BoB. **Supplementary Figures 1, 2** depict the dominance of seasonality over the interannual changes. Since the increase in Chl-a is significantly smaller, it is compelling to note that the Chl-a concentration in BoB is increasing in recent decade relative to the previous decades. In contrast, AS exhibits a reduction in magnitude of Chl-a compared to the earlier years. As the trend of AOD is increasing in both the basins, it is noteworthy that the atmospheric deposition plays a major role in modifying the Chl-a concentration over the NIO with negative correlation of -0.61



in AS and -0.52 in BoB, respectively; consistent with previous studies (e.g., Patra et al., 2007).

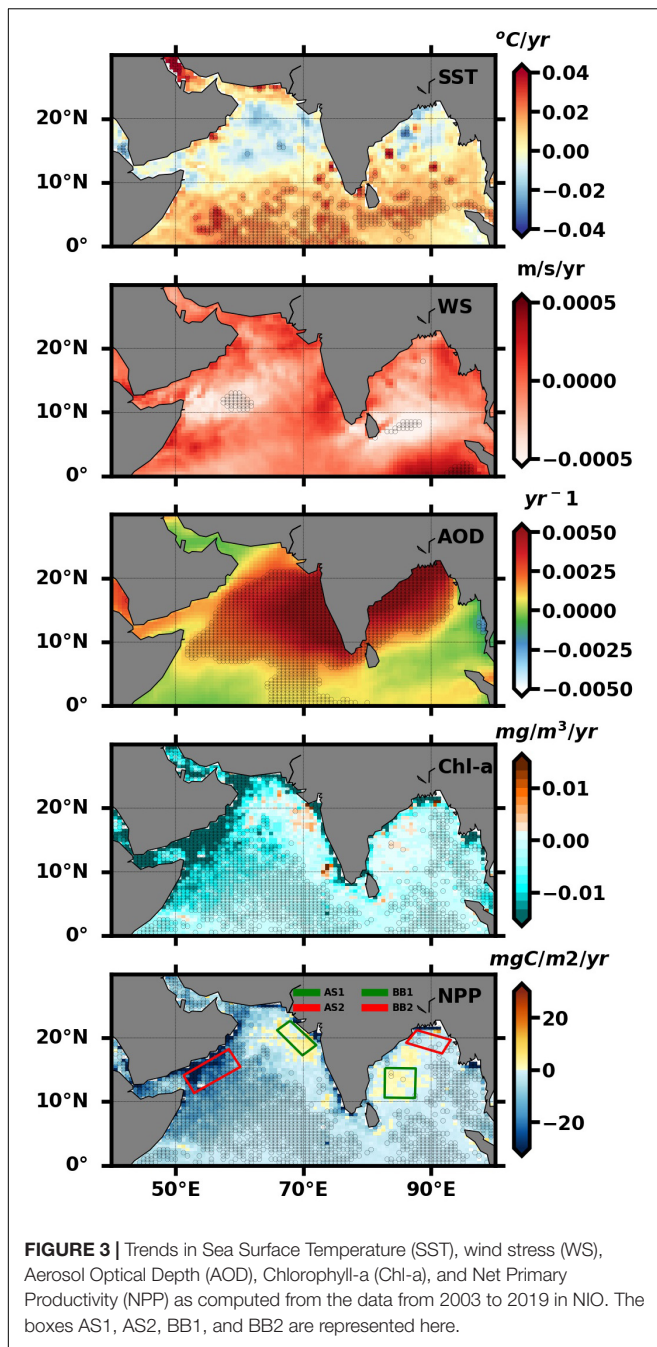
Supplementary Figures 3, 4 show the interannual variability of Chl-a and SST in the concentric box like regions in AS and BoB. As discussed earlier, the warming of oceans is associated with lower Chl-a, whereas insignificant warming regions exhibit enhanced Chl-a. Therefore, we have also examined the interannual variability of Chl-a and WS over AS and BoB (**Supplementary Figures 5, 6**). The analyses reveal that SST has negative and WS has a positive feedback on Chl-a abundance with a dominant seasonal cycle. The analyses show that SST and Chl-a have negative feedback, but WS and Chl-a have positive feedback with distinct seasonal cycles. It is evident from the analysis that the phytoplankton concentration is influenced by the combined effects of these physical processes. As observed in the case of Chl-a and AOD, the seasonal cycle is predominant in AS than the annual cycle in SST and WS. Some of the previous studies also suggest atmospheric deposition as a reason for increasing phytoplankton biomass along the eastern coast of India during the winter monsoon (e.g., Yadav et al., 2016) and it could be one of the factors for increasing Chl-a and NPP in BoB in recent years, such as 2018 and 2019.

Statistical Analysis on Interannual Variability of NPP

In addition to the analysis using the concentric box regions, we have also used a box plot to depict the interannual variability of Chl-a, NPP, SST, and WS. We have considered four regions (AS1,

AS2, BB1, and BB2) based on positive/negative spatial trends of NPP (**Figure 3**) in AS and BoB, respectively, and these regions are marked in **Figure 3**.

The box plots and annual mean (black line) of AS1 and BB1 along with 95 % confidence intervals of basin average (AS and BoB) are presented in **Figure 4**. The year-wise distribution is represented using different boxes with the median in the middle, and whiskers of the corresponding boxes represent the maximum and minimum excluding outliers. The analyses reveal the overall decrease in NPP and Chl-a. The large dispersions are exhibited more over AS (larger box regions) than that in BoB (smaller box regions). From 2003 to 2014, the median values decreased and reached up to 0.25 mg/m^3 in 2014. The median value increased in 2015 and is about 0.5 mg/m^3 , and further decreases until 2019. NPP exhibits a similar pattern as for Chl-a. The median values are below $750 \text{ mgC/m}^2/\text{day}$ in AS1 and below $500 \text{ mgC/m}^2/\text{day}$ in BB1. Nevertheless, it is shown that the long-term trends in both basins show a decrease in Chl-a and NPP. The Chl-a are generally positively skewed (mean values greater than median) although they exhibit noticeable variability in distribution in AS1. They are positively skewed in 2003 and 2004, and remain symmetric (equal distribution) up to 2008. Furthermore, they are positively skewed up to 2016 and negatively skewed (mean less than median) in 2017, but are again positively skewed (mean less than median) in 2018 and 2019. Similar distribution is depicted in the case of NPP. The Chl-a and NPP values are much smaller in BB1 although it exhibits an upward skewness. The distribution of SST exhibits negative skewness in



AS1 and BB1. The variability of WS is prominent in BB1 and is positively skewed in AS1 and BB1. There are outliers in WS that indicate tendency toward maximum extremes, as shown in AS1 and BB1. AOD also exhibits positive skewness with outliers tending toward maximum extremes.

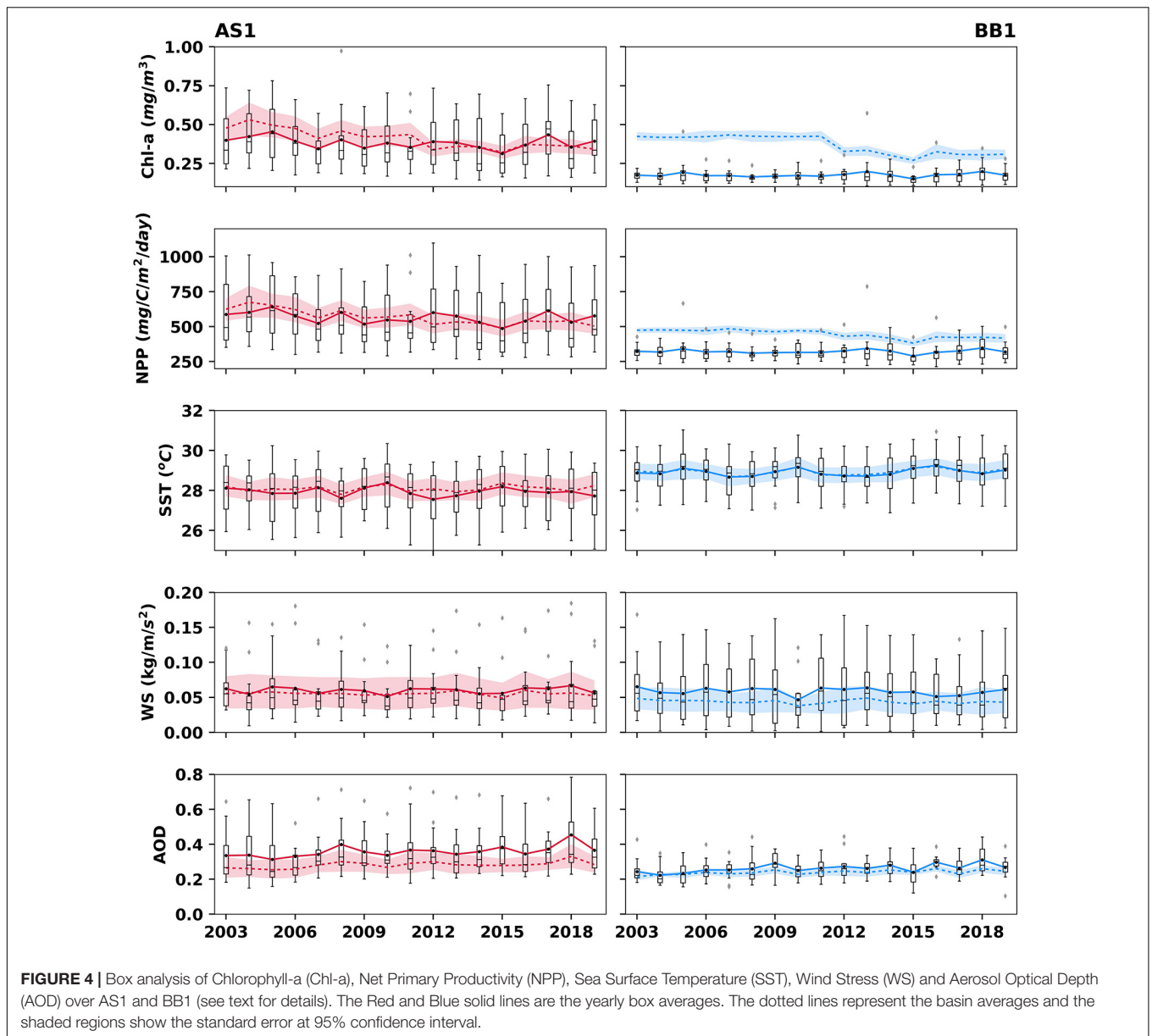
The distribution of Chl-a, SST, WS, AOD, and NPP in AS2 and BB2 are shown in **Supplementary Figure 7**. The Chl-a, NPP, WS, AOD, and SST exhibit upward skewness in AS2. The SST depicts a downward skewness in BB2, whereas Chl-a, AOD, WS and NPP show small variability in BB1. Both basins show comparable changing patterns of the previously mentioned variables. The

annual mean of Chl-a shows a similar pattern until 2007 where there is a sudden decline in 2007, but increases in 2008. There was an abrupt decline with very small Chl-a (0.25 mg/m^3) values in 2014, but increased thereafter. The NPP distribution also reveals decline as observed in Chl-a. The mean Chl-a and NPP values in AS1 are about 0.38 mg/m^3 and $564.4 \text{ mg/C/m}^2/\text{day}$ in AS1. The dip observed in 2007 is complemented with a rise in SST with respect to 2006. There was a drop in SST in 2008. The abrupt drop in SST was observed in 2012 and it further increased in 2015. The mean SST in AS1 is about 27.94°C and about 28.91°C in BB1. WS shows very small changes when compared to other variables. The mean AOD concentrations in AS1 and BB1 are about 0.35 and 0.26, respectively.

We have calculated the correlation of Chl-a with respect to SST, NPP, and WS. The correlation and lag/lead between the variables are estimated at 95 % confidence level. The phase relationships between the variables can help identify the underlying causes (Shafeeque et al., 2017) and therefore, we have used the phase relationships to find the correlation between the variables. The Chl-a is positively correlated with WS and NPP with correlations of 0.90 and 0.98 in AS1 and 0.66 and 0.97 in BB1. The Chl-a is negatively correlated with AOD and SST with correlations -0.66 and -0.83 in AS1 and -0.69 and -0.75 in BB1. All the correlations are statistically significant. The correlation values along with lag/lead information are presented in **Supplementary Table 3**.

Impact of COVID-19 Lockdown on NPP

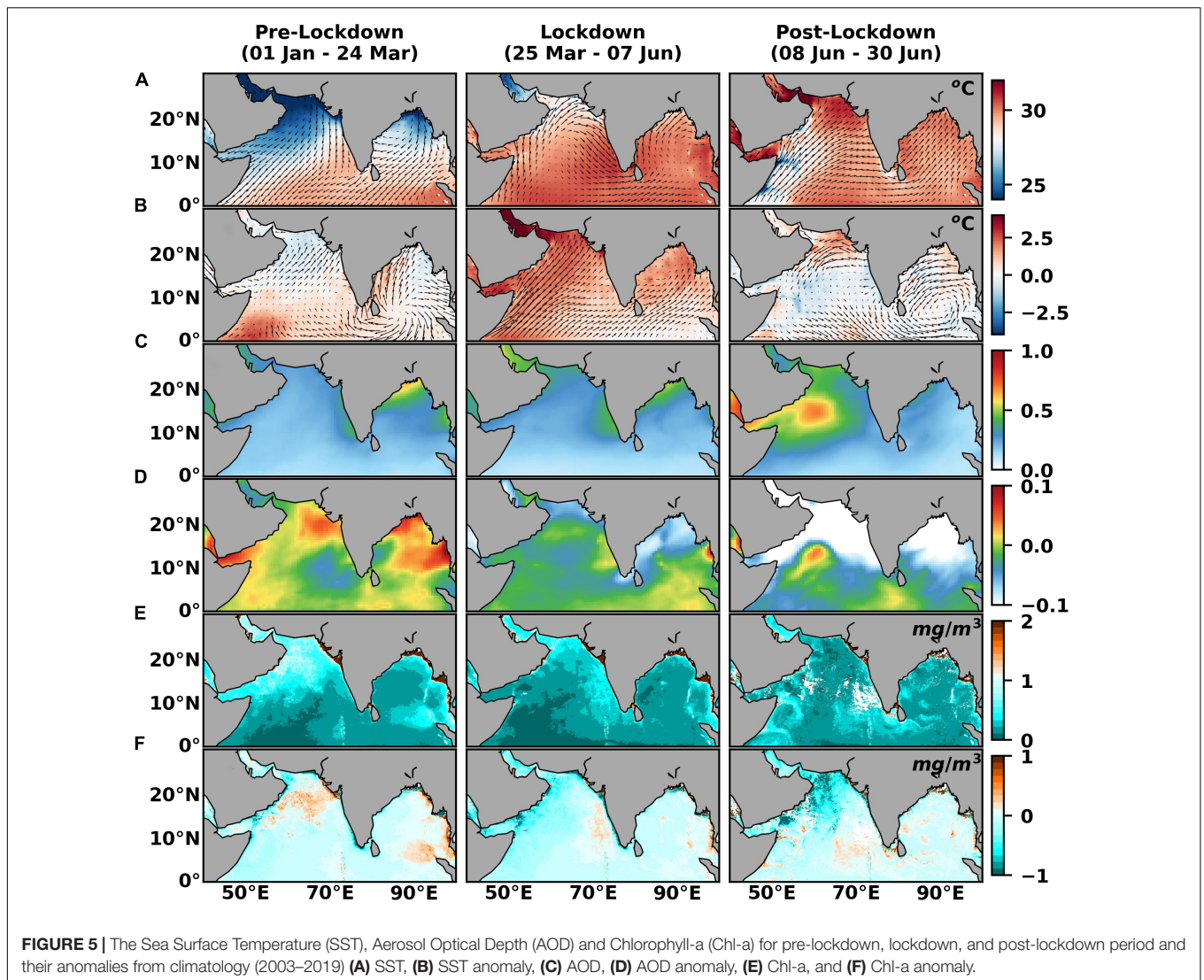
The worldwide spread of contagious disease caused by SARS-CoV-2 compelled governments to declare countrywide lockdown. The immediate consequence of the lockdown was that there were considerable changes in the anthropogenic inputs to the atmosphere (Kumar, 2020; Singh and Chauhan, 2020). Although there are studies on the impact of lockdown on atmospheric pollution and air quality, no study is performed yet to examine the impact of lockdown on oceanic processes. To understand the impact of lockdown on the oceanic Chl-a and NPP, we analyzed the data for three periods: pre-lockdown, lockdown, and post-lockdown. **Figure 5A** shows the variability of SST overlaid with 10 m surface wind vectors for these periods and the corresponding anomaly (**Figure 5B**) for the year 2020 from the 17-year climatology (2003–2019). The analysis shows a warming (positive anomaly) in the lockdown period throughout the northern BoB and AS, although no significant change is observed in the southern BoB and AS. This might be probably due to the increased oceanic heat content in the northern AS and BoB (Gnanaseelan et al., 2017; Cheng et al., 2021). It is challenging to hold lockdown responsible for this warming as the ocean responds a little later than the atmosphere and it is already known that NIO is warming at alarming rates. In spite of lockdown and lower emissions due to COVID-19, the upper ocean warms up to 2,000 m (Cheng et al., 2021), making 2020 one of the hottest years. However, the SST anomaly over the lockdown period reveals a warming episode over the northern regions of AS and BoB, while the wind anomalies do not show any significant change over the period.



Most Indian states and metropolitan cities exhibited negative AOD anomalies during the lockdown period compared to the pre-lockdown period as reported in Singh and Chauhan (2020), and the reasons might be restrictions in movement, lesser emissions due to shutdown/limited working of industries and reduction in human activities due to complete shutdown leading to lesser concentration of aerosols. Our analysis (**Figures 5C,D**) also shows a higher AOD in the pre-lockdown period, further dips in the lockdown period. There are negative anomalies of AOD during the lockdown period. During the post-lockdown period, the anomalies are positive. The effect of aerosols is such that it helps in backscattering which leads to cooling in the atmosphere whereas strong aerosols absorb radiation which facilitates warming. The reduction of aerosols in turn leading to reduction of backscattering might be the reason for

warming during the lockdown period. **Figures 5E,F** represent the Chl-a for the periods and the corresponding anomaly. During the lockdown period, a positive anomaly was observed in the eastern AS. The anomaly was negative in the western and northern AS, which coincides with the warming there. The BoB does not exhibit any significant changes in the Chl-a. The statistical significance of anomalies is calculated using the student *t*-test. The significance of anomalies is provided in **Supplementary Table 4**.

To ensure that the changes are related to or can be related to impacts of COVID-19 lockdown, we made a similar analysis for the year 2018 over the same dates such as pre-lockdown, lockdown, and post-lockdown and are shown in **Supplementary Figure 8**. The anomalous warming observed in 2020 is not replicated in 2018 in the lockdown period. However, AOD shows



a positive anomaly in AS and BoB in contrast to the negative anomaly observed in 2020 in the lockdown period. Although it is difficult to confirm that these effects are only due to the lockdown, the negative anomaly of AOD in 2020 might be due to the reduced anthropogenic activities during the lockdown period. The Chl-a distribution does not show reasonable changes in comparison to 2020.

To make a comprehensive assessment, we look into the temporal variability of AOD, Chl-a, and NPP in 2020. To understand the difference more efficiently, we compared it with climatology (Figure 6). AOD values remain well below the climatology in all the three boxes in AS during the lockdown period in comparison to pre and post-lockdown periods. The seasonal peaks during MAM and JJAS in 2020 are below the climatology which could be attributed to the imposed lockdown. However, the Chl-a values do not exhibit much changes during the lockdown period and further increases in the post-lockdown period. The peaks are observed in August and September. The Chl-a is maximum during JJAS, and therefore, these changes may

not be directly related to post-lockdown. AOD is higher in the post-lockdown period in Box 1 in BoB, whereas in Box 2 and Box 3, it is lower than the climatological mean.

The temporal analysis of NPP (Figure 6) shows that NPP is very small in the lockdown period in AS, whereas there is a sharp decline in NPP during the lockdown period in Boxes 2 and 3 in BoB. However, this decline was not observed for Chl-a (Figure 6). The NPP depends on PAR, SST and the length of the day, and might be one of these factors during the lockdown might have contributed to the smaller NPP in MAM. We have not analyzed each of these factors separately, instead we analyzed the available data to examine the impact of COVID-19 lockdown on NPP. We observe that SST is higher during the period when the NPP is smaller (Supplementary Figure 9).

Similarly, we also made the monthly analysis over the concentric boxes over the same period but for the year 2018, to examine whether the changes are associated with COVID-19 lockdown (Supplementary Figure 10). The peaks of AOD generally present in MAM and JJAS are less than the climatology

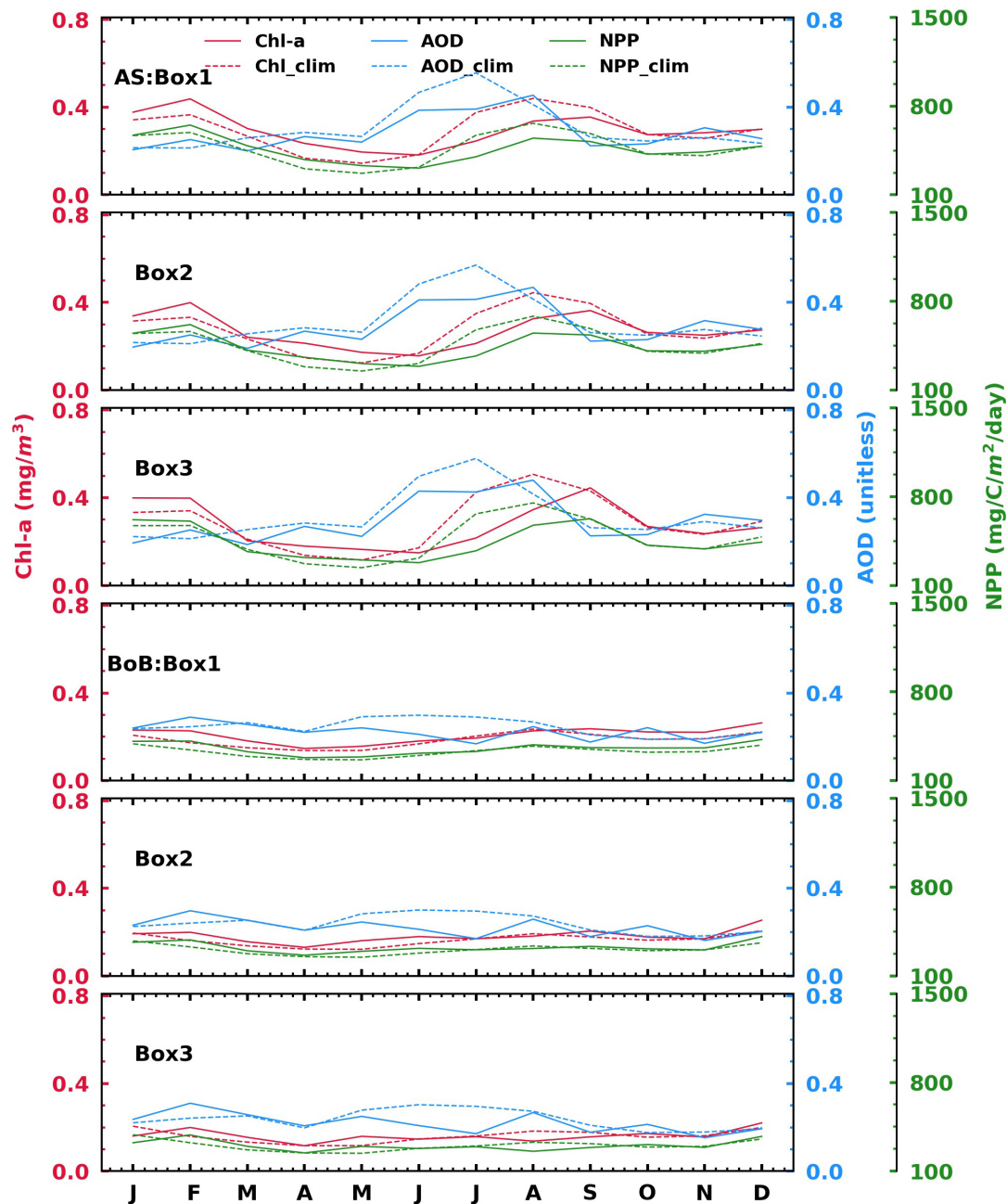


FIGURE 6 | The temporal variation of Aerosol Optical Depth (AOD), Chlorophyll-a (Chl-a), and Net Primary Productivity (NPP) for 2020.

in 2020, but it exceeds the climatology in 2018. Chl-a values are higher than climatology in 2018, whereas they are lesser than climatology in 2020. The negative anomaly of Chl-a and AOD with respect to the climatological mean, however, is not significant during the lockdown period. The analyses suggest that the lockdown can be one of the reasons for the lesser AOD and less Chl-a in both basins.

The monthly analysis of NPP and AOD in concentric boxes for the same period in 2018, is carried out to check whether

these changes are associated with the lockdown. The results are presented in **Supplementary Figure 11**. It shows lower values of NPP than the climatology during the lockdown period of 2020, but the same feature was not observed in 2018 and they are higher than the climatology. This again indicates the impact of COVID-19 lockdown on the open ocean primary production. The increase in productivity in the monsoon months observed in 2018 is also not observed in 2020, which might also be connected to the COVID-19 lockdown.

CONCLUSION

We use satellite and reanalysis data for 17 years across all seasons to examine the interannual variability of NPP and the impact of lockdown on NPP. One of the major reasons for choosing OC-CCI Chl-a data is the improved coverage, particularly during the monsoon periods. The main aim of the study is the estimation of variability of primary productivity in NIO and examine them in the context of COVID-19 lockdown. We find that Chl-a has positive correlation with NPP and wind, but a negative correlation with SST with a time lag, consistent with known seasonal changes in winds and SST.

We analyze the response of NIO to the lockdown implemented in connection with COVID-19 pandemic. Our analysis suggests that AOD shows an increasing trend over AS and BoB, while Chl-a and NPP show a decreasing trend in AS, particularly in the southern AS where an increasing trend in SST is observed; implying the reduction in oceanic productivity with global ocean warming. In BoB, the central regions show an increasing trend of Chl-a and NPP, which is also evident in the interannual variability of Chl-a, AOD, and NPP. The seasonal cycle of all variables is more prominent in AS than that in BoB. Although Chl-a throughout AS shows higher values than that in BoB, there is a small increase in Chl-a over BoB compared to the previous years. Our study also shows an increase in AOD over both basins, and the increasing trend of NPP coincides with a decreasing trend in SST in the same region. The NPP is very small during the lockdown period in 2020, which is also complemented by an increase in SST during the lockdown period. AOD is relatively lower during the lockdown period, which may be due to the effect of lockdown. The decrease in AOD in the lockdown period in 2020 is not observed in 2018. Although it is difficult to confirm, the analyzed results suggest that the changes in AOD, SST and NPP in 2020 are very likely due to the lockdown. Analyses of ship or onboard measurements may strengthen our conclusions, yet the initial analyses do exhibit changes related to lockdown such as the increase in aerosols, and SST, and thus reduction in NPP. Henceforth, our analyses provide new insights into the

impact of the changes in atmospheric input on the oceanic primary productivity.

DATA AVAILABILITY STATEMENT

The original contributions presented in the study are included in the article/**Supplementary Material**, further inquiries can be directed to the corresponding author.

AUTHOR CONTRIBUTIONS

JK conceived the idea and supervised the research. NS did the analyses and drew the figures. JK and NS wrote the first draft which was subsequently modified by inputs from JK, RP, KC, and AC. All authors contributed to the article and approved the submitted version.

ACKNOWLEDGMENTS

The authors would like to thank Head CORAL, the Director of Indian Institute of Technology Kharagpur (IIT Kgp), Sponsored Research and Industrial Consultancy of IIT Kgp, and Indian National Centre for Ocean Information Services, Ministry of Earth Sciences, Hyderabad (INCOIS, O-MASCOT project). The authors would also like to thank Ocean Color Climate Change Initiative (OC-CCI) for providing us with the daily chlorophyll-a data, NASA Ocean Color and European Centre for Medium-Range Weather Forecast (ECMWF) for the various data sets used in this study. This is INCOIS contribution number 431.

SUPPLEMENTARY MATERIAL

The Supplementary Material for this article can be found online at: <https://www.frontiersin.org/articles/10.3389/fmars.2021.669415/full#supplementary-material>

REFERENCES

- Anderson, D. M., and Prell, W. L. (1992). The structure of the southwest monsoon winds over the Arabian Sea during the late Quaternary: observations, simulations, and marine geologic evidence. *J. Geophys. Res. Ocean* 97, 15481–15487. doi: 10.1029/92jc01428
- Anderson, D. M., Brock, J. C., and Prell, W. L. (1992). Physical upwelling processes, upper ocean environment and the sediment record of the southwest monsoon. *Geol. Soc. London Spec. Publ.* 64, 121–129. doi: 10.1144/gsl.sp.1992.064.01.08
- Banerjee, P., and Prasanna Kumar, S. (2014). Dust-induced episodic phytoplankton blooms in the Arabian Sea during winter monsoon. *J. Geophys. Res. Ocean* 119, 7123–7138. doi: 10.1002/2014jc010304
- Beaufort, L., Lancelot, Y., Camberlin, P., Cayre, O., Vincent, E., Bassinot, F., et al. (1997). Insolation cycles as a major control of equatorial Indian Ocean primary production. *Science* 278, 1451–1454. doi: 10.1126/science.278.5342.1451
- Behrenfeld, M. J., and Falkowski, P. G. (1997). Photosynthetic rates derived from satellite-based chlorophyll concentration. *Limnol. Oceanogr.* 42, 1–20. doi: 10.4319/lo.1997.42.1.0001
- Caley, T., Malaizé, B., Zaragosi, S., Rossignol, L., Bourget, J., Eynaud, F., et al. (2011). New Arabian Sea records help decipher orbital timing of Indo-Asian monsoon. *Earth Planet. Sci. Lett.* 308, 433–444. doi: 10.1016/j.epsl.2011.06.019
- Chakraborty, K., Lotliker, A. A., Gupta, G. V. M., Narayanan Nampoothiri, S. V., Paul, A., Ghosh, J., et al. (2020). Assessment of an ocean-ecosystem model in simulating the Indian coastal marine ecosystem dynamics. *J. Oper. Oceanogr.* 2020, 1–19. doi: 10.1080/1755876x.2020.1843298
- Chakraborty, K., Valsala, V., Gupta, G. V. M., and Sarma, V. (2018). Dominant biological control over upwelling on pCO₂ in sea east of Sri Lanka. *J. Geophys. Res. Biogeosci.* 123, 3250–3261. doi: 10.1029/2018jg004446
- Chavez, F. P., Messié, M., and Pennington, J. T. (2011). Marine Primary Production in Relation to Climate Variability and Change. *Ann. Rev. Mar. Sci.* 3, 227–260. doi: 10.1146/annurev.marine.010908.163917
- Cheng, L., Abraham, J., Trenberth, K. E., Fasullo, J., Boyer, T., Locarnini, R., et al. (2021). Upper ocean temperatures hit record high in 2020. *Adv. Atmos. Sci.* 38, 523–530. doi: 10.1007/s00376-021-0447-x
- Chowdary, J. S., Parekh, A., Ojha, S., and Gnanaseelan, C. (2015). Role of upper ocean processes in the seasonal SST evolution over tropical Indian Ocean in

- climate forecasting system. *Clim. Dyn.* 45, 2387–2405. doi: 10.1007/s00382-015-2478-4
- Cropp, R. A., Gabric, A. J., McTainsh, G. H., Braddock, R. D., and Tindale, N. (2005). Coupling between ocean biota and atmospheric aerosols: dust, dimethylsulphide, or artifact?. *Global Biogeochem. Cycles* 19:GB4002.
- Fathrio, I., Iizuka, S., Manda, A., Kodama, Y.-M., Ishida, S., Moteki, Q., et al. (2017). Assessment of western Indian Ocean SST bias of CMIP5 models. *J. Geophys. Res. Ocean* 122, 3123–3140. doi: 10.1002/2016jc012443
- Field, C. B., Behrenfeld, M. J., Randerson, J. T., and Falkowski, P. (1998). Primary production of the biosphere: integrating terrestrial and oceanic components. *Science* 281, 237–240. doi: 10.1126/science.281.5374.237
- Findlater, J. (1969). A major low-level air current near the Indian Ocean during the northern summer. *Q. J. R. Meteorol. Soc.* 95, 362–380. doi: 10.1002/qj.49709540409
- Gallissai, R., Peters, F., Volpe, G., Basart, S., and Baldasano, J. M. (2014). Saharan dust deposition may affect phytoplankton growth in the Mediterranean Sea at ecological time scales. *PLoS One* 9:e110762. doi: 10.1371/journal.pone.0110762
- GCOS (2011). Systematic Observation Requirements from Satellite-Based Data Products for Climate 2011 Update. Supplemental Details to the Satellite-Based Component of the “Implementation Plan for the Global Observing System for Climate in Support of the UNFCCC. *GCOS Rep.* 154, 138.
- Global Modeling and Assimilation Office (GMAO) (2015). *MERRA-2 instM_2d_gas_Nx: 2d, Monthly mean, Instantaneous, Single-Level, Assimilation, Aerosol Optical Depth Analysis V5.12.4*. Greenbelt: Goddard Earth Sciences Data and Information Services Center.
- Gnanaseelan, C., Roxy, M. K., and Deshpande, A. (2017). “Variability and trends of sea surface temperature and circulation in the Indian Ocean,” in *Observed climate variability and change over the Indian Region*, eds M. Rajeevan and S. Nayak (Singapore: Springer), 165–179. doi: 10.1007/978-981-10-2531-0_10
- Goddard Space Flight Center (NASA), Ocean Ecology Laboratory, Ocean Biology Processing Group, and Moderate-resolution Imaging Spectroradiometer (MODIS). (2018). *Aqua Photosynthetically Available Radiation Data; 2018 Reprocessing*. Greenbelt: NASA Goddard Space Flight Center, doi: 10.5067/AQUA/MODIS/L3M/PAR/2018 Accessed on 06/25/2021.
- Goes, J. I., Thoppil, P. G., do, R., Gomes, H., and Fasullo, J. T. (2005). Warming of the Eurasian landmass is making the Arabian Sea more productive. *Science* 308, 545–547. doi: 10.1126/science.1106610
- Gower, J. F. R., Doerffer, R., and Borstad, G. A. (1999). Interpretation of the 685 nm peak in water-leaving radiance spectra in terms of fluorescence, absorption and scattering, and its observation by MERIS. *Int. J. Remote Sens.* 20, 1771–1786. doi: 10.1080/014311699212470
- Gregg, W. W., Casey, N. W., and McClain, C. R. (2005). Recent trends in global ocean chlorophyll. *Geophys. Res. Lett.* 32:L03606.
- Hersbach, H., Bell, B., Berrisford, P., Hirahara, S., Horányi, A., Muñoz-Sabater, J., et al. (2020). The ERA5 global reanalysis. *Q. J. R. Meteorol. Soc.* 146, 1999–2049.
- Hossain, M. S., Sarker, S., Sharifuzzaman, S. M., and Chowdhury, S. R. (2020). Primary productivity connects hilsa fishery in the Bay of Bengal. *Sci. Rep.* 10:5659.
- Howarth, R. W. (1988). Nutrient limitation of net primary production in marine ecosystems. *Annu. Rev. Ecol. Syst.* 19, 89–110. doi: 10.1146/annurev.es.19.110188.000513
- Hu, C., Muller-Karger, F. E., Taylor, C. J., Carder, K. L., Kelble, C., Johns, E., et al. (2005). Red tide detection and tracing using MODIS fluorescence data: a regional example in SW Florida coastal waters. *Remote Sens. Environ.* 97, 311–321. doi: 10.1016/j.rse.2005.05.013
- IPCC (2018). “Global Warming of 1.5°C. An IPCC Special Report on the impacts of global warming of 1.5°C above pre-industrial levels and related global greenhouse gas emission pathways,” in *The Context of Strengthening the Global Response to the Threat of Climate Change, Sustainable Development, and Efforts to Eradicate Poverty*, eds V. Masson-Delmotte, P. Zhai, H.-O. Portner, D. Roberts, and J. Sheea (Geneva: World Meteorological Organization), 32.
- Jickells, T. D., An, Z. S., Andersen, K. K., Baker, A. R., Bergametti, C., Brooks, N., et al. (2005). Global iron connections between desert dust, ocean biogeochemistry, and climate. *Science* 308, 67–71. doi: 10.1126/science.1105959
- Jordi, A., Basterretxea, G., Tovar-Sánchez, A., Alastuey, A., and Querol, X. (2012). Copper aerosols inhibit phytoplankton growth in the Mediterranean Sea. *Proc. Natl. Acad. Sci. U. S. A.* 109, 21246–21249. doi: 10.1073/pnas.1207567110
- Joseph, P. V., Sooraj, K. P., and Rajan, C. K. (2006). The summer monsoon onset process over South Asia and an objective method for the date of monsoon onset over Kerala. *Int. J. Climatol.* 26, 1871–1893. doi: 10.1002/joc.1340
- Käse, L., and Geuer, J. K. (2018). “Phytoplankton responses to marine climate change—an introduction,” in *YOUARES 8—Oceans Across Boundaries: Learning from each other*, eds S. Jungblut, V. Liebich, and M. Bode (Cham: Springer), 55–71. doi: 10.1007/978-3-319-93284-2_5
- Keen, T. R., Kindle, J. C., and Young, D. K. (1997). The interaction of southwest monsoon upwelling, advection and primary production in the northwestern Arabian Sea. *J. Mar. Syst.* 13, 61–82. doi: 10.1016/s0924-7963(97)00003-1
- Kumar, M. D., Naqvi, S. W. A., Jayakumar, D. A., George, M. D., Narvekar, P. V., and de Sousa, S. N. (1995). Carbon dioxide and nitrous oxide in the North Indian Ocean. *Curr. Sci.* 69, 672–678.
- Kumar, S. (2020). Effect of meteorological parameters on spread of COVID-19 in India and air quality during lockdown. *Sci. Total Environ.* 745:141021. doi: 10.1016/j.scitotenv.2020.141021
- Kumar, S., Ramesh, R., Sardesai, S., and Sheshshayee, M. S. (2004). High new production in the Bay of Bengal: possible causes and implications. *Geophys. Res. Lett.* 31:L18304.
- Kuttippurath, J., Murasingh, S., Stott, P. A., Sarojini, B. B., Jha, M. K., Kumar, P., et al. (2021a). Observed rainfall changes in the past century (1901–2019) over the wettest place on Earth. *Environ. Res. Lett.* 16:24018.
- Kuttippurath, J., Sunanda, N., Martin, M. V., and Chakraborty, K. (2021b). Tropical storms trigger phytoplankton blooms in the deserts of north Indian Ocean. *npj Clim. Atmos. Sci.* 4:11. doi: 10.1038/s41612-021-00166-x
- Kuttippurath, J., and Raj, S. (2021). Two decades of aerosol observations by AATSR, MISR, MODIS and MERRA-2 over India and Indian Ocean. *Remote Sens. Environ.* 257:112363. doi: 10.1016/j.rse.2021.112363
- Le Mézo, P., Beaufort, L., Bopp, L., Braconnot, P., and Kageyama, M. (2017). From monsoon to marine productivity in the Arabian Sea: insights from glacial and interglacial climates. *Clim. Past* 13, 759–778. doi: 10.5194/cp-13-759-2017
- Lee, C. M., Jones, B. H., Brink, K. H., and Fischer, A. S. (2000). The upper-ocean response to monsoonal forcing in the Arabian Sea: seasonal and spatial variability. *Deep Sea Res. II Top. Stud. Oceanogr.* 47, 1177–1226. doi: 10.1016/s0967-0645(99)00141-1
- Levitus, S., Antonov, J. I., Boyer, T. P., and Stephens, C. (2000). Warming of the world ocean. *Science* 287, 2225–2229. doi: 10.1126/science.287.5461.2225
- Li, F., and Ramanathan, V. (2002). Winter to summer monsoon variation of aerosol optical depth over the tropical Indian Ocean. *J. Geophys. Res. Atmos.* 107, AAC2-1–AAC2-13.
- Madhuratap, M., Kumar, S. P., Bhattathiri, P. M. A., Kumar, M. D., Raghukumar, S., Nair, K. K. C., et al. (1996). Mechanism of the biological response to winter cooling in the northeastern Arabian Sea. *Nature* 384, 549–552. doi: 10.1038/384549a0
- Mahowald, N. M., Scanza, R., Brahney, J., Goodale, C. L., Hess, P. G., Moore, J. K., et al. (2017). Aerosol deposition impacts on land and ocean carbon cycles. *Curr. Clim. Change E. Rep.* 3, 16–31. doi: 10.1007/s40641-017-0056-z
- Mallet, M., Chami, M., Gentili, B., Sempéré, R., and Dubuisson, P. (2009). Impact of sea-surface dust radiative forcing on the oceanic primary production: a 1D modeling approach applied to the West African coastal waters. *Geophys. Res. Lett.* 36:L15828.
- Martin, J. H., Coale, K. H., Johnson, K. S., Fitzwater, S. E., Gordon, R. M., Tanner, S. J., et al. (1994). Testing the iron hypothesis in ecosystems of the equatorial Pacific Ocean. *Nature* 371, 123–129.
- McCreary, J. P., Murtugudde, R., Vialard, J., Vinayachandran, P. N., Wiggert, J. D., Hood, R. R., et al. (2009). Biophysical processes in the Indian Ocean. *Indian Ocean Biogeochem. Process. Ecol. Var.* 185, 9–32. doi: 10.1029/2008gm000768
- Moore, C. M., Mills, M. M., Arrigo, K. R., Berman-Frank, I., Bopp, L., Boyd, P. W., et al. (2013). Processes and patterns of oceanic nutrient limitation. *Nat. Geosci.* 6, 701–710.
- Moorthy, K. K., Babu, S. S., and Satheesh, S. K. (2003). Aerosol spectral optical depths over the Bay of Bengal: role of transport. *Geophys. Res. Lett.* 30:1249.
- Murtugudde, R., and Busalacchi, A. J. (1999). Interannual variability of the dynamics and thermodynamics of the tropical Indian Ocean. *J. Clim.* 12, 2300–2326. doi: 10.1175/1520-0442(1999)012<2300:ivotda>2.0.co;2
- Patra, P. K., Behera, S. K., Herman, J. R., Maksyutov, S., Akimoto, H., and Yamagata, T. (2005). The Indian summer monsoon rainfall: interplay of coupled dynamics,

- radiation and cloud microphysics. *Atmos. Chem. Phys.* 5, 2181–2188. doi: 10.5194/acp-5-2181-2005
- Patra, P. K., Kumar, M. D., Mahowald, N., and Sarma, V. (2007). Atmospheric deposition and surface stratification as controls of contrasting chlorophyll abundance in the North Indian Ocean. *J. Geophys. Res. Ocean* 112:C05029.
- Paytan, A., Mackey, K. R. M., Chen, Y., Lima, I. D., Doney, S. C., Mahowald, N., et al. (2009). Toxicity of atmospheric aerosols on marine phytoplankton. *Proc. Natl. Acad. Sci. U. S. A.* 106, 4601–4605. doi: 10.1073/pnas.0811486106
- Prakash, P., Prakash, S., Rahaman, H., Ravichandran, M., and Nayak, S. (2012). Is the trend in chlorophyll-a in the Arabian Sea decreasing?. *Geophys. Res. Lett.* 39:L23605.
- Prasanna Kumar, S., Muraleedharan, P. M., Prasad, T. G., Gauns, M., Ramaiah, N., De Souza, S. N., et al. (2002). Why is the Bay of Bengal less productive during summer monsoon compared to the Arabian Sea?. *Geophys. Res. Lett.* 29, 88–81. doi: 10.1029/2002GL016013
- Prasanna Kumar, S., Ramaiah, N., Gauns, M., Sarma, V., Muraleedharan, P. M., Raghukumar, S., et al. (2001). Physical forcing of biological productivity in the Northern Arabian Sea during the Northeast Monsoon. *Deep Sea Res. II Top. Stud. Oceanogr.* 48, 1115–1126. doi: 10.1016/S0967-0645(00)00133-8
- Prasanna Kumar, S., Roshin, R. P., Narvekar, J., Kumar, D., and Vivekanandan, E. (2010). What drives the increased phytoplankton biomass in the Arabian Sea?. *Curr. Sci.* 99, 101–106.
- Prospero, J. M., Ginoux, P., Torres, O., Nicholson, S. E., and Gill, T. E. (2002). Environmental characterization of global sources of atmospheric soil dust identified with the Nimbus 7 Total Ozone Mapping Spectrometer (TOMS) absorbing aerosol product. *Rev. Geophys.* 40, 1–31.
- Rahaman, H., Srinivasu, U., Panickal, S., Durgadoo, J. V., Griffies, S. M., Ravichandran, M., et al. (2020). An assessment of the Indian Ocean mean state and seasonal cycle in a suite of interannual CORE-II simulations. *Ocean Model.* 145:101503. doi: 10.1016/j.ocemod.2019.101503
- Ramachandran, S., and Jayaraman, A. (2002). Premonsoon aerosol mass loadings and size distributions over the Arabian Sea and the tropical Indian Ocean. *J. Geophys. Res. Atmos.* 107, AAC 1–1–AAC 1–21.
- Ramanathan, V., Crutzen, P. J., Lelieveld, J., Mitra, A. P., Althausen, D., Anderson, J., et al. (2001). Indian Ocean Experiment: an integrated analysis of the climate forcing and effects of the great Indo-Asian haze. *J. Geophys. Res. Atmos.* 106, 28371–28398. doi: 10.1029/2001JD900133
- Roxy, M. K., Ritika, K., Terray, P., Murtugudde, R., Ashok, K., and Goswami, B. N. (2015). Drying of Indian subcontinent by rapid Indian Ocean warming and a weakening land-sea thermal gradient. *Nat. Commun.* 6:7423.
- Satheesh, S. K., Moorthy, K. K., Kaufman, Y. J., and Takemura, T. (2006). Aerosol optical depth, physical properties and radiative forcing over the Arabian Sea. *Meteorol. Atmos. Phys.* 91, 45–62. doi: 10.1007/s00703-004-0097-4
- Sathyendranath, S., Jackson, T., Brockmann, C., Brotas, V., Calton, B., Chuprin, A., et al. (2020). *Global Chlorophyll-a Data Product s Gridded on a Sinusoidal Projection, Version 4.2*. Chilton: Centre for Environmental Data Analysis.
- Schott, F. A., Xie, S.-P., and McCreary, J. P. Jr. (2009). Indian Ocean circulation and climate variability. *Rev. Geophys.* 47:RG1002.
- Shafeeqe, M., Sathyendranath, S., George, G., Balchand, A. N., and Platt, T. (2017). Comparison of seasonal cycles of phytoplankton chlorophyll, aerosols, winds and sea-surface temperature off Somalia. *Front. Mar. Sci.* 4:386. doi: 10.3389/fmars.2017.00386
- Shenoi, S. S. C., Shankar, D., and Shetye, S. R. (2002). Differences in heat budgets of the near-surface Arabian Sea and Bay of Bengal: implications for the summer monsoon. *J. Geophys. Res. Ocean* 107, 1–5.
- Singh, R. P., and Chauhan, A. (2020). Impact of lockdown on air quality in India during COVID-19 pandemic. *Air Qual. Atmos. Health* 13, 921–928. doi: 10.1007/s11869-020-00863-1
- Subramanian, V. (1993). Sediment load of Indian rivers. *Curr. Sci.* 64, 928–930.
- Vinayachandran, P. N., and Shetye, S. R. (1991). The warm pool in the Indian Ocean. *Proc. Indian Acad. Sci. Planet. Sci.* 100, 165–175.
- Vinayachandran, P. N., Chauhan, P., Mohan, M., Nayak, S. (2004). Biological response of the sea around Sri Lanka to summer monsoon. *Geophys. Res. Lett.* 31:L01302. doi: 10.1029/2003GL018533
- Wang, M., Son, S., and Shi, W. (2009). Evaluation of MODIS SWIR and NIR-SWIR atmospheric correction algorithms using SeaWiFS data. *Remote Sens. Environ.* 113, 635–644. doi: 10.1016/j.rse.2008.11.005
- Webb, P. (2019). *Introduction to oceanography*. Bristol: Roger Williams University.
- Webster, P. J., Magana, V. O., Palmer, T. N., Shukla, J., Tomas, R. A., Yanai, M. U., et al. (1998). Monsoons: processes, predictability, and the prospects for prediction. *J. Geophys. Res. Ocean* 103, 14451–14510. doi: 10.1029/97jc02719
- Werdell, P. J., Franz, B. A., Bailey, S. W., Feldman, G. C., Boss, E., Brando, V. E., et al. (2013). Generalized ocean color inversion model for retrieving marine inherent optical properties. *Appl. Opt.* 52, 2019–2037. doi: 10.1364/ao.52.002019
- Wielicki, B. A., Barkstrom, B. R., Baum, B. A., Charlock, T. P., Green, R. N., Kratz, D. P., et al. (1998). Clouds and the Earth's Radiant Energy System (CERES): algorithm overview. *IEEE Trans. Geosci. Remote Sens.* 36, 1127–1141.
- Wiggert, J. D., Hood, R. R., Banse, K., and Kindle, J. C. (2005). Monsoon-driven biogeochemical processes in the Arabian Sea. *Prog. Oceanogr.* 65, 176–213. doi: 10.1016/j.pocean.2005.03.008
- Yadav, K., Sarma, V., Rao, D. B., and Kumar, M. D. (2016). Influence of atmospheric dry deposition of inorganic nutrients on phytoplankton biomass in the coastal Bay of Bengal. *Mar. Chem.* 187, 25–34. doi: 10.1016/j.marchem.2016.10.004
- Zhou, X., Duchamp-Alphonse, S., Kageyama, M., Bassinot, F., Beaufort, L., and Colin, C. (2020). “Primary productivity dynamics in the northeastern Bay of Bengal over the last 26,000 years,” in *EGU General Assembly Conference Abstracts, 10253*. Munich: European Geosciences Union.

Conflict of Interest: The authors declare that the research was conducted in the absence of any commercial or financial relationships that could be construed as a potential conflict of interest.

Publisher's Note: All claims expressed in this article are solely those of the authors and do not necessarily represent those of their affiliated organizations, or those of the publisher, the editors and the reviewers. Any product that may be evaluated in this article, or claim that may be made by its manufacturer, is not guaranteed or endorsed by the publisher.

Copyright © 2021 Sunanda, Kuttippurath, Peter, Chakraborty and Chakraborty. This is an open-access article distributed under the terms of the Creative Commons Attribution License (CC BY). The use, distribution or reproduction in other forums is permitted, provided the original author(s) and the copyright owner(s) are credited and that the original publication in this journal is cited, in accordance with accepted academic practice. No use, distribution or reproduction is permitted which does not comply with these terms.